Microstructures of 4H–SiC single crystals deformed under very high stresses

2002 J. Phys.: Condens. Matter 14 12961

(http://iopscience.iop.org/0953-8984/14/48/338)

INSTITUTE OF PHYSICS PUBLISHING JOURNAL OF PHYSICS: CONDENSED MATTER

J. Phys.: Condens. Matter **14** (2002) 12961–12966 PII: S0953-8984(02)53987-4

Microstructures of 4H–SiC single crystals deformed under very high stresses

J L Demenet[1,7], J Rabier[1], X Milhet[2], M H Hong[3,4], P Pirouz[3], I Stretton[5] and P Cordier[5,6]

[1] Laboratoire de Métallurgie Physique, UMR 6630 CNRS, Université de Poitiers, BP 179, 86962 Futuroscope Chasseneuil Cedex, France
[2] Laboratoire de Mécanique et de Physique des Matériaux, UMR 6617 CNRS, ENSMA, 1 avenue Clément Ader, BP 40109, 86961 Futuroscope Chasseneuil Cedex, France
[3] Department of Materials Science and Engineering, Case Western Reserve University, Cleveland, OH 44106-7204, USA
[4] Rolling Products Research Group, POSCO Technical Research Lab, 699 Kumhodong, Kwangyang Cheonam 545-090, Korea
[5] Bayerisches Geoinstitut, Universität Bayreuth, 95440 Bayreuth, Germany
[6] Laboratoire de Structure et Propriétés de l'Etat Solide, ESA CNRS 8008, Université des Sciences et Technologies de Lille, Villeneuve d'Ascq, France

E-mail: Jean.Luc.Demenet@univ-poitiers.fr

Received 27 September 2002
Published 22 November 2002
Online at stacks.iop.org/JPhysCM/14/12961

Abstract
The microstructure of 4H–SiC single crystals deformed under very high stresses and at low temperature ($T \leqslant 350\,^\circ$C) have been analysed by transmission electron microscopy. Depending on deformation conditions, large stacking faults, weakly dissociated perfect dislocations and possibly undissociated perfect dislocations have been observed. From these results, it appears that the nucleation of partial dislocations, which is a limiting process in deformation of 4H–SiC below $\sim$1000 °C, can be helped by very high stress. Consequently, it is not excluded that a deformation mechanism by undissociated perfect dislocations can take place under very high stress, as observed in Si and GaAs.

1. Introduction

The plasticity of semiconductors has been extensively studied, mainly in elemental (Si) and III–V compounds (GaAs, InP, InSb, . . .) which can be grown as very high quality crystals. By contrast, because SiC single crystals—which are IV–IV compounds—were not available until recently, there were only a few reports on deformation tests for this material. The main work in this field has been performed by Fujita *et al* (1987) on Acheson-grown 6H–SiC crystals over the temperature range of 1300–1600 °C. The recent availability on the commercial market of

[7] Author to whom any correspondence should be addressed.

large single crystals grown by the modified-Lely method has made it possible to study the plasticity of this material. Deformation tests over large ranges of temperature and strain rates have been performed on 6H– and 4H–SiC by Samant *et al* (1998) and Demenet *et al* (2000).

As for other semiconductors, due to the directional bonding between the atoms, SiC is ductile at high temperatures and brittle at low temperatures. The transition temperature is in the range of 1000–1100 °C, depending on the strain rate. It appears that below the transition temperature, only leading partial dislocations with large stacking faults behind are observed, whereas above the transition temperature, deformation occurs by perfect, weakly dissociated dislocations. Based on these observations, a model has been proposed that describes the transition temperature as the onset of the nucleation of trailing partials in this material and to correspond to the brittle-to-ductile temperature (Pirouz *et al* 1999, 2001). In addition, it is suggested that at low temperatures the stress could be high enough to reduce significantly the enthalpy energy for nucleation of trailing partials and to promote the occurrence of perfect dislocations.

This paper deals with preliminary transmission electron microscopy (TEM) observations of 4H–SiC single crystals deformed under very high stresses and at low temperatures that are far below the transition temperature.

2. Experimental procedures

A single crystal ingot of 4H–SiC was grown along the [0001] direction at Cree Research Inc., using the technique of modified sublimation (seeded Lely). The as-received crystal was pale and transparent with a nitrogen content of about 2×10^{18} cm^{-3}. After orientation by x-ray diffraction, parallelepiped-shaped samples were cut from the bulk crystal with the basal (0001) plane at 45° to the compression axis. After cutting, the faces of each sample were ground using a 20 μm diamond impregnated disc followed by 9 and 3 μm diamond paste polish. Three samples were deformed under the following conditions:

(i) Sample A was introduced into a hot isostatic press (HIP) for 4 h at 300 °C under a pressure of 200 MPa of argon gas.

(ii) Sample B was deformed using a Paterson press at 350 °C and $\dot{\varepsilon} = 1.1 \times 10^{-5}$ s^{-1}, under a Ar-gas confining pressure of 300 MPa. The engineering stress level at the end of the test was 2160 MPa corresponding to a permanent strain of 1.2%.

(iii) Sample C was deformed at room temperature (RT) in an anisotropic multi-anvil apparatus at a confining pressure of 5 GPa. With this technique it is possible to get a large deviatoric stress superimposed onto a known large hydrostatic pressure (Cordier and Rubie 2001). As a consequence of the design of the confining solid medium, the deviatoric stress is unknown, but the deformation strain rate can be estimated to be about 5×10^{-5} s^{-1}.

After deformation, thick slices were cut from each sample with a diamond saw. A slice parallel to (0001) was extracted from sample A. For experiments using the Paterson press and the multi-anvil apparatus, samples B and C were embedded in a metallic jacket, which prevented the basal plane from being localized at the end of the experiments. For this reason, the slices for the TEM were cut perpendicularly to the compression axis. Subsequently, the slices were ground with an impregnated diamond disc down to a thickness of 80 μm, dimpled down to a thickness of 20 μm, and ion-milled to electron transparency. TEM experiments were performed on a Philips CM20 electron microscope operating at an accelerating voltage of 200 kV and using a double-tilt specimen holder.

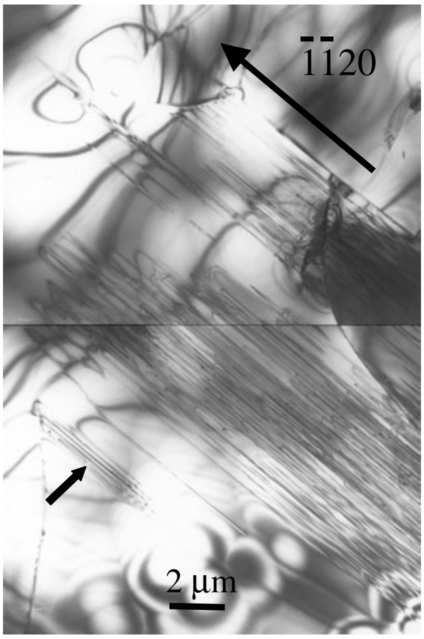

Figure 1. The microstructure of sample A deformed by HIP at 300 °C. Half-loops of dislocations elongated in the $[\bar{1}\bar{1}20]$ direction are evidenced. Bright field, $g = \bar{1}\bar{1}20$, electron beam $B = 0001$. A microcrack from where a few dislocations were emitted is shown by the arrow.

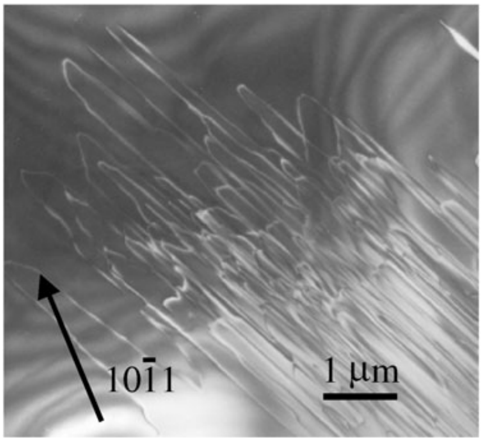

Figure 2. The same zone as in figure 1. A dark-field micrograph of the dislocation configuration taken with $g = 10\bar{1}1$ near the $[\bar{1}012]$ zone axis showing the stacking fault contrasts.

3. Results

3.1. Sample A

Figure 1 shows a typical example of the dislocation microstructure produced in sample A deformed by HIP. The micrograph was taken with the reflection $g = \bar{1}\bar{1}20$ and the incident beam direction $B = 0001$. In this bright field TEM micrograph, a very high density of dislocations is observed. The dislocations emanate from the bottom right-hand side and form half-loops elongated along the $[\bar{1}\bar{1}20]$ direction. The nucleation site of these dislocation loops has not been determined due to the too-large thickness of the thin foil which prevents analysis of this zone. Dislocation multiplication may result from the anisotropy of the material, or the nucleation of dislocations may be promoted under pressure from heterogeneities in the bulk, like cavities, micropipes (Pirouz 1998), or other pre-existing or deformation-induced defects. Indeed, in addition to dislocations, some cracks propagating without a preferential direction are observed. For example, some dislocations emanate from the microcrack that is shown by the arrow in figure 1.

Basically, dislocation half-loops are composed of perfect, weakly dissociated dislocations. This is evidenced in figure 2, imaged with $g = 10\bar{1}1$ near the $[\bar{1}012]$ zone axis, showing the typical stacking fault contrasts. The Burger's vectors of partial dislocations bounding the stacking faults were determined using the standard weak-beam $g \cdot b = 0$ invisibility criterion. The outside dislocations are in contrast with the reflections $g = \bar{1}\bar{1}20$ and $\bar{2}110$ and are out of contrast with the reflection $g = 1\bar{2}10$. Their Burger's vector is $b_L = 1/3[\bar{1}010]$. On the other hand, the inside dislocations are out of contrast with $g = \bar{2}110$ and in contrast with

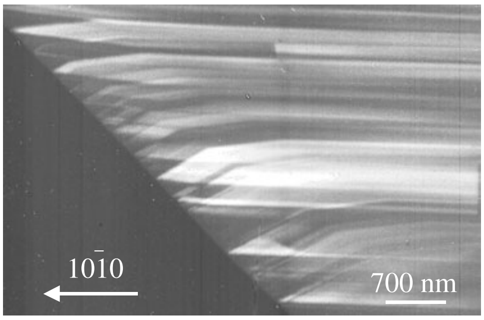

Figure 3. The observation of large stacking faults in sample B deformed at $T = 350\,^{\circ}\mathrm{C}$ and $\dot{\varepsilon} = 1.1 \times 10^{-5}\ \mathrm{s}^{-1}$ using the Paterson press. The confining pressure was 300 MPa with $\boldsymbol{g} = 10\bar{1}0$.

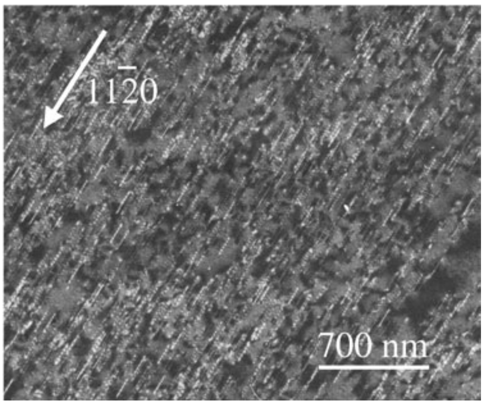

Figure 4. The microstructure of sample C deformed at RT in an anisotropic multi-anvil apparatus under 5 GPa. Dark field $\boldsymbol{g} = 11\bar{2}0$ and electron beam $\boldsymbol{B} = 1\bar{1}00$.

$\boldsymbol{g} = \bar{1}\bar{1}20$ and $\bar{2}110$. Their Burger's vector is $\boldsymbol{b}_T = 1/3[0\bar{1}10]$. The outside and inside partial dislocations with a stacking fault in between result from the dissociation in the basal plane of a perfect $\boldsymbol{b}_p = 1/3[\bar{1}\bar{1}20]$ dislocation, following the reaction

$$\boldsymbol{b}_p(1/3[\bar{1}\bar{1}20]) \rightarrow \boldsymbol{b}_L(1/3[\bar{1}010) + \boldsymbol{b}_T(1/3[0\bar{1}10]).$$

All the half-loops in figures 1 and 2 have the same Burger's vector and are elongated along the screw direction, proving a lower mobility of this segment. It can be noticed that the stacking fault width is very inhomogeneous. Although, in some cases it is impossible to measure the separation width of the partials because of limited TEM resolution, measured values fall between 10 and 100 nm. This is in agreement with the distance of ~50 nm measured in 4H–SiC deformed at 1300 °C and corresponding to a stacking fault energy of $\sim 15\ \mathrm{mJ\ m^{-2}}$ (Hong *et al* 2000). From these results, the deformation of 4H–SiC using HIP experiments appears to be governed by perfect, weakly dissociated dislocations.

3.2. Sample B

A typical aspect of the microstructure of sample B deformed using the Paterson press, is shown in figure 3. The stacking fault contrasts are evidenced using $\boldsymbol{g} = 10\bar{1}0$ as the diffraction vector. All explored areas of the thin foil present the same feature, and no perfect dislocations have been observed. Observations in the basal plane were not possible owing to tilting limitations, as discussed in section 2. Finally, it appears that the microstructure is built with large stacking faults, presumably lying in the basal plane. These observations are consistent with those reported on samples that are deformed in a conventional way at higher temperatures (Pirouz *et al* 2001).

3.3. Sample C

Figure 4 shows the microstructure of sample C that is deformed at RT in an anisotropic multi-anvil apparatus. At the end of the experiment, the sample was broken in several pieces so that the thin foil for the TEM observations extracted from one of those pieces was randomly oriented. In figure 4, the basal plane is seen edge on. Very short segments of dislocations

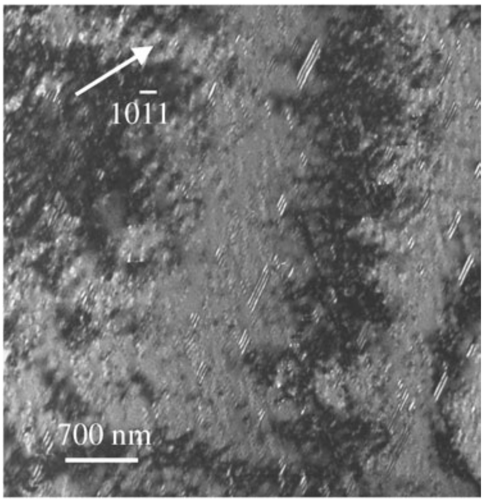

Figure 5. The same zone as in figure 4 with dark field $g = 10\bar{1}1$ and electron beam $B = \bar{1}101$. A few large stacking faults are visible.

lying along the trace of the basal plane are visible with $g = 11\bar{2}0$. These segments are out of contrast when imaging with $g = 0004$: they belong to one of the glide systems of the (0001) plane. Tilting the specimen as much as possible toward (0001), i.e. ($\bar{1}101$) at 30° from the basal plane, most of those dislocations are seen out of contrast using $g = 10\bar{1}1$ whereas a few large stacking faults are observed (figure 5). These contrast experiments are consistent with the fact that most of the dislocations nucleated at RT have $1/3[1\bar{2}10]$ Burger's vectors and they are perfect or weakly dissociated dislocations.

4. Discussion

In the present study, three 4H–SiC samples were deformed under harsh and very different conditions. Except for the case of sample B, the stress level on the samples was unknown due to the particular deformation conditions. However, the qualitative preliminary results presented here are discussed in the light of existing models.

The lowest temperature at which 4H–SiC can be deformed by conventional deformation tests without catastrophic failure is 550 °C (Samant *et al* 1998). The superimposition of a 300 MPa confining pressure allowed us to deform the material at a lower temperature: 350 °C ($\dot{\varepsilon} = 1.1 \times 10^{-5}$ s^{-1}). The resulting microstructure is composed of large stacking faults, comparable to Samant's observations at 550 °C. However, it must be pointed out that the thin foil orientation prevented us from checking if deformation occurs by emission of leading partials with large stacking faults behind, or by widely dissociated perfect dislocations.

A model, suggested by Pirouz *et al* (1999, 2001) describes the transition temperature T_c observed in $\ln(\tau_y) = f(1/T)$ curves as the lower temperature at which trailing partials can be nucleated and associated with leading partials, yielding a ductile behaviour of the material by repetitive emission of dissociated perfect dislocations acting in the same plane. Below T_c, only leading partial dislocations are nucleated and glide occurs on parallel slip planes. These dislocations contribute to a very limited extent to the straining of the crystal, since the sources become inoperative after they emit only one partial dislocation. However, according to the model, the effective activation energy is lowered by the applied resolved shear stress. Under very high stresses, such as those applied at low temperature, the activation enthalpy could be lowered sufficiently to make nucleation of the trailing partial dislocation possible, resulting in leading–trailing pairs of partials. The observation of perfect dislocation half-loops weakly dissociated in sample A supports such a hypothesis.

Suzuki *et al* (1999) succeeded in deforming dislocation-free GaAs below 300 K (down to 77 K) under a confining pressure of 400 MPa. TEM observations show a microstructure consisting of predominantly perfect screw dislocations, whereas at higher temperature (RT) deformation occurs by dissociated dislocations or by twinning (Rabier and Boivin 1990). Perfect dislocations have also been evidenced in dislocation-free silicon by Rabier and Demenet (2000) deformed at 150 °C and RT using the same multi-anvil apparatus as that used in the present study. Those two materials, and possibly other III–V compounds, suffer a change in their deformation mechanism, from dissociated dislocations at moderate temperature and stress to perfect, undissociated dislocations at low temperature and very high stress. The case of 4H–SiC is still under investigation. In the high temperature–low stress regime, i.e. above T_c, deformation occurs by emission and propagation of correlated leading–trailing pairs of partial dislocations. Below the transition temperature, in a temperature and stress range that still needs to be determined, the effective enthalpy energy for the nucleation of trailing partials becomes too high and only leading partials participate in the limited deformation of the material. Under very high stress, trailing partials can again be nucleated and deformation occurs by leading–trailing pairs of partial dislocations. It is not excluded that, as reported in Si and GaAs, a different plastic deformation mechanism by perfect dislocations occurs in 4H–SiC at RT under very high stress. Complementary observations and experiments are needed to confirm the preliminary results on the behaviour of 4H–SiC under very high stress as presented in this paper.

Acknowledgments

Thanks are due to Dr Calvin Carter Jr of Cree Research, Inc., for providing a single-crystal ingot of 4H–SiC. High-pressure experiments (Paterson press and multi-anvil press) were performed at the Bayerisches Geoinstitut under the EU 'IHP—Access to Research Infrastructures' Programme (contract no HPRI-1999-CT-00004 to D C Rubie).

References

Cordier P and Rubie D 2001 *Mater. Sci. Eng.* A **309–310** 38
Demenet J L, Hong M H and Pirouz P 2000 *Scr. Mater.* **43** 865
Fujita S, Maeda K and Hyodo S 1987 *Phil. Mag.* A **55** 203
Hong M H, Samant A V and Pirouz P 2000 *Phil. Mag.* A **80** 919
Pirouz P 1998 *Phil. Mag.* A **78** 727
Pirouz P, Samant A V, Hong M H, Moulin A and Kubin L P 1999 *J. Mater. Res.* **14** 2783
Pirouz P, Demenet J L and Hong M H 2001 *Phil. Mag.* A **81** 1207
Rabier J and Boivin P 1990 *Phil. Mag.* A **61** 673
Rabier J and Demenet J L 2000 *Phys. Status Solidi* b **222** 63
Samant A V, Zhou W L and Pirouz P 1998 *Phys. Status Solidi* a **166** 155
Suzuki T, Yasutomi T, Tokuoka T and Yonenaga I 1999 *Phil. Mag.* A **79** 2637